

Morphosynthesis of star-shaped titania-silica shells

Dirk Volkmer, Stefano Tugulu, Matthias Fricke, Tim Nielsen

Angaben zur Veröffentlichung / Publication details:

Volkmer, Dirk, Stefano Tugulu, Matthias Fricke, and Tim Nielsen. 2003. "Morphosynthesis of star-shaped titania-silica shells." *Angewandte Chemie International Edition* 42 (1): 58–61.
<https://doi.org/10.1002/anie.200390051>.

Nutzungsbedingungen / Terms of use:

licgercopyright

Dieses Dokument wird unter folgenden Bedingungen zur Verfügung gestellt: / This document is made available under these conditions:

Deutsches Urheberrecht

Weitere Informationen finden Sie unter: / For more information see:

<https://www.uni-augsburg.de/de/organisation/bibliothek/publizieren-zitieren-archivieren/publiz/>



Morphosynthesis of Star-Shaped Titania–Silica Shells**

Dirk Volkmer, Stefano Tugulu, Matthias Fricke, and Tim Nielsen*

Biomining organisms such as diatoms or radiolaria develop intricately shaped inorganic casings mainly consisting of amorphous silica.^[1] In spite of the ubiquity of these organisms the morphogenetic foundations of cell development yielding a species-specific shell design are poorly understood. However, a few details of silica metabolic

pathways in diatoms and other silicifying organisms have been discovered recently, including hitherto unknown classes of enzymes (silicateins^[2]) and peptides (silaffins,^[3] frustulins,^[4] pleuralins (formerly HEPs),^[5] SP41^[6]) being either associated with silicic acid polycondensation, precipitation, or shell development.

The unicellular diatoms are particularly interesting model organisms that may give rise to novel biomimetic strategies for producing complex, hierarchically structured materials.^[7] Shell development in diatoms occurs within a highly specialized membrane compartment, the so-called silica deposition vesicle (SDV).^[8] There is still much debate about the processes that serve to mould the SDV into its final shape.^[9] SDVs occur among a broad range of protists (testate amoebae, heliozoa, and radiolaria), which hints to a common secretory mechanism for the production of siliceous structures.^[10] Clearly, the formation of hierarchically structured silicified cell walls involves distinct differentiation/growth steps at the characteristic length scales, ranging from nano- to micron-sized structures, and thus a distinction between micro- and macromorphogenesis has been proposed recently.^[11]

Herein we present our first endeavors to set up a biomimetic model system of shell formation in unicellular organisms such as diatoms or radiolaria. The model system consists of a surfactant-stabilized oil droplet which is microinjected into an aqueous solution. The oil droplet contains small amounts of a monomeric metal oxide precursor, which starts to hydrolyze when brought in contact to the aqueous phase, finally leading to formation of a mineralized shell at the oil–water interface. The progress of mineralization is monitored in situ by means of video microscopy. This relatively simple system was chosen because it shows decisive features characteristic of biological systems. It has a primitive silicon “metabolism” that liberates monomeric silicic acid from a masked storage deposit. The release of hydrolytically unstable metal oxide precursors occurs at a membrane-type surface. The oil droplet dimensions are comparable to the sizes of typical silicifying unicellular organisms (10–100 μm). Owing to the limited amount of metal oxide precursor contained within the oil droplet, the shell formation process is intrinsically self-terminating. Finally, but most importantly, appropriately chosen organic additives dissolved in the oil phase (or the aqueous solution, respectively) may induce dynamic self-organization processes that ultimately lead to formation of discrete hollow shells of complex shapes.

Among the many experiments conducted so far, our attention was attracted by a particular system which leads to the morphosynthesis of discrete star-shaped shells bearing a striking resemblance to the silicified skeletons of radiolaria. The basic reaction system consists of a small droplet of chlorocyclohexane that contains arachidic acid ($c = 42.4 \text{ mM}$).^[12] The aqueous phase consists of a highly diluted solution of cetyltrimethylammonium bromide (CTAB, $c = 55.6 \text{ }\mu\text{M}$). Upon microinjection, the surface of the oil droplet starts to become corrugated within a few minutes (Figure 1). We observe the growth of small liquid-filled spines extruding from the surface of the oil droplet. The spines sometimes reach a length of approximately 90 μm , while typical diameters range from 3 to 15 μm .

[*] Dr. D. Volkmer, S. Tugulu
University of Bielefeld
Faculty of Chemistry, AC1
33501 Bielefeld (Germany)
Fax: (+49) 521-106-6003
E-mail: dirk.volkmer@uni-bielefeld.de
M. Fricke, Dr. T. Nielsen
University of Bielefeld
Faculty of Physics, D3 (Germany)

[**] This work was supported by the Deutsche Forschungsgemeinschaft (DFG Schwerpunktprogramm 1117 “Prinzipien der Biomineralisation”; DFG grant Vo 829/2-1). D.V. thanks the DFG for a habilitation scholarship (DFG grant Vo 829/1-1).

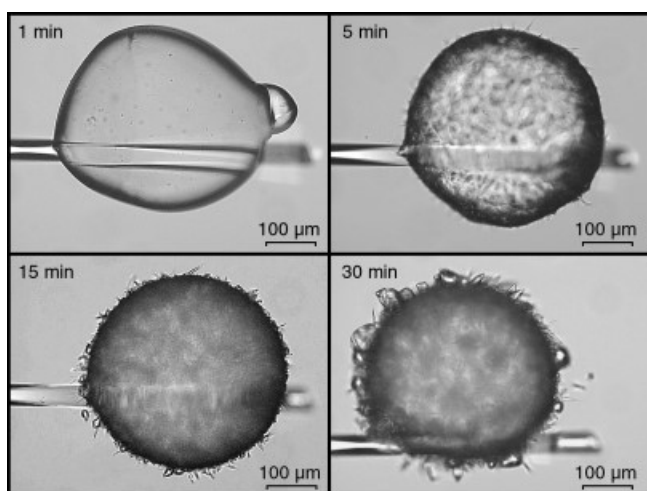


Figure 1. Timelapse recording of the spontaneous emulsification of a chlorocyclohexane droplet containing arachidic acid ($c=42.4$ mM) after microinjection into an aqueous solution of CTAB ($c=55.6$ μ M) (bright-field optical micrographs).

Upon reaching a critical size, the spines start to tie up and form a corona of submicroscopic droplets around the original oil droplet. The dissipation process continues until most of the original droplet is divided into smaller size microemulsion droplets which subsequently start to spread out into the aqueous solution. Similar dynamic self-organization processes have been reported and are commonly referred to as *spontaneous emulsification*.^[13] It is noteworthy that under the chosen experimental conditions the emulsification process only occurs when oppositely charged surfactants are used within the two different liquid phases. Substituting arachidic acid with arachidyl alcohol, for instance, or omitting one surfactant, does not lead to spontaneous emulsification at all. Thus it is anticipated that electrostatic interactions between the oppositely charged surfactants contribute a great deal to the driving force of the process.^[14]

The challenge here was to couple the mineralization process to the spontaneous dissipation of the oil droplet while preserving the metastable star-shape morphology. This is achieved by proper choice of the metal oxide precursor being added to the oil phase and careful adjustment of surfactant concentrations. We were first unable to establish a simple silica-based model system that would have led to robust silica shells at ambient conditions (i.e. room temperature, aqueous solution at $\text{pH} \approx 7$) in a suitable time frame.^[15] A major improvement was achieved by employing titania or mixtures of titania/silica precursors that are hydrolytically less stable than typical silica precursors (tetramethoxysilane (TMOS), tetraethoxysilane (TEOS)) used within initial experiments (see Supporting Information).^[16] Using admixtures of tetra-*tert*-butyl orthotitanate (TBOT) we are able to produce smooth and robust, mineralized shells at the oil–water interface within a few minutes to hours, depending on the experimental conditions.

Figure 2 shows a timelapse recording of optical micrographs similar to those in Figure 1. The oil droplet now contains a small amount of titania precursor (TBOT). Again, formation of a star-shape morphology is observed, but in

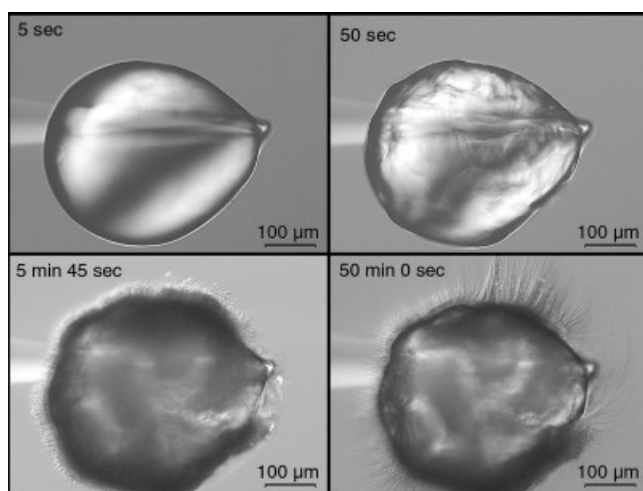


Figure 2. Timelapse recording of spine formation of a chlorocyclohexane droplet containing arachidic acid ($c=42.4$ mM) and tetra-*tert*-butyl orthotitanate (TBOT, 4 wt%) after microinjection into an aqueous solution of CTAB ($c=0.556$ mM) (differential interference contrast optical micrographs).

contrast to the system without metal oxide precursor, the dissipation process becomes frozen at an intermediate stage after a few minutes. A closer inspection of the particles thus obtained shows that the mineralized surface consists of thin hollow spines (av. diameter: 1 μ m) that may grow up to a length of some 100 μ m. The star-shaped titania particles are completely stable if kept in aqueous solution but they rapidly decompose upon drying in air. Attempts to preserve the morphology by freeze-drying procedures have failed so far. Scanning electron micrographs of freeze-dried samples reveal hollow mineralized shells (av. wall thickness ≈ 1 μ m), while the characteristic spines have completely disappeared. According to scanning electron micrographs the remaining mineral shell consists of a mesoporous network of partially coalesced titania colloid particles with typical diameters ranging from 40–70 nm. The fact that the spines are completely lost during sample drying points to a low mineral content of these structural elements.

A systematic variation of surfactant and precursor concentrations, respectively, shows that the genesis of star-shaped titania particles is a highly concentration-dependent process: The most uniform particles are obtained at a TBOT starting concentration of about 4 wt%. At TBOT contents below 3 wt%, the dissipation process is slowed down compared to the precursor-free system, but eventually leads to formation of microemulsion droplets; TBOT contents exceeding 5 wt%, in contrast, yield massive mineral shells encompassing the oil droplet, which lack radial undulations.

The putative composition of spines that develop during emulsification led us to employ fluorescence microscopy to answer the principle question, as to whether or not the growing spines are filled with organic solvent. By adding a hydrophobic fluorescent probe (coumarin 153) to the chlorocyclohexane solution, we were able to image the time-dependent spatial distribution of the immiscible liquid phases by real-time laser-scanning microscopy. We employed a novel multibeam two-photon microscope with diffraction limited

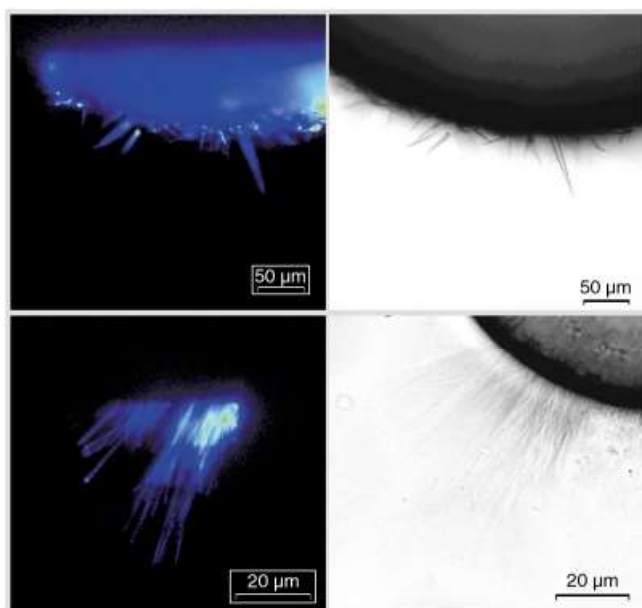


Figure 3. Fluorescence images (left side) and bright-field optical micrographs (right side) taken from the oil droplet periphery during spine development. Pictures correspond to the system lacking precursor (top row) and containing a titania precursor (bottom row). The spines and the laser-dissected fraction of the oil droplet appear in blue or green colors against the dark (nonfluorescent) background.

three-dimensional spatial resolution and fast scanning capability (frame rates up to 60 Hz) to record optical sections of the droplets and the spines.^[17] The fluorescence signal is taken as a measure of the coumarin concentration and can be used to visualize the distribution of the organic solvent.

Figure 3 shows representative fluorescence images (left side) as opposed to bright field optical micrographs (right side) taken from the droplet periphery during spine development. The pictures in the top row correspond to the system without precursor. The spines and the laser-dissected fraction of the oil droplet appear in blue or green colors against the dark (nonfluorescent) background. Colors represent different fluorescence intensity levels. It is clearly seen that the fluorescence intensity is uniform throughout the main body of the oil droplet and the spines, which is indicative of a homogeneous distribution of the fluorescent probe and the organic solvent, suggesting a continuous transition between oil droplet and spines. A similar picture is gained from the fluorescence images of the precursor-containing system (Figure 3, bottom), which shows a comparably uniform fluorescence throughout the thin spines radiating from the surface of the oil droplet. We conclude that spine formation in both systems is governed by a similar self-organization process that involves surfactant-mediated development of interface curvature between two immiscible liquid phases.

Based on these experiments we currently rule out that complex surfactant aggregates, for example, surfactant multilayer tubules,^[18] are involved in spine formation as found, for instance, in fluid-rod structures of hydrated solid lecithin surfaces (“myelin figures”). By employing single droplet microinjection experiments, we were able to narrow the optimum concentration range of chemical components. As a

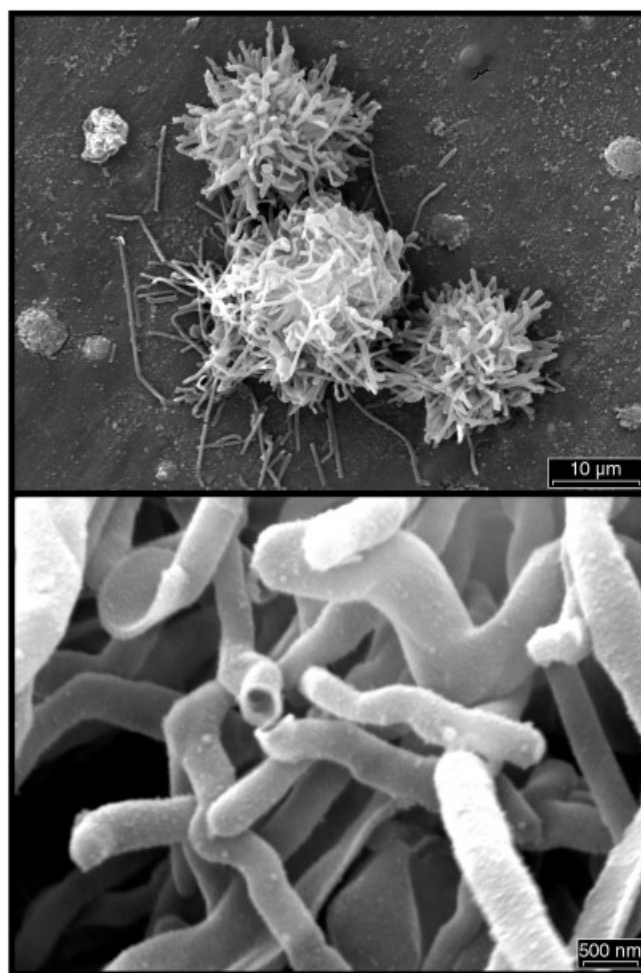


Figure 4. Scanning electron micrographs of star-shaped titania-silica shells from bulk sample preparation procedures. Top: Typical morphology of an air-dried sample demonstrating the robust nature of the mineralized shells. Bottom: Fractured sample indicating the hollow tubular nature of mineralized spines.

remaining challenge we finally transferred our insights gained from video microscopy investigations to a technically simple bulk sample preparation procedure. This was achieved by adding a silica precursor (TMOS) to the oil phase or the aqueous solution. Mechanically robust mineralized star-shaped particles are then obtained by adding a small volume of chlorocyclohexane, which contains a TBOT/TMOS precursor, to a pre-hydrolyzed aqueous solution of TMOS. The suspension is gently shaken a few times in a closed vial and the suspension is left to stand quiescent for a few days, while sedimentation of the emulsion droplets occurs. Light microscopic examination of the particles that have settled at the bottom of the vial reveal high yields of star-shaped particles that possess a narrow size distribution with average diameters ranging from 10–100 μm. The fraction of particles with small diameters (10–20 μm) are found to be quite robust which simplifies preparation of samples suitable for electron microscopic investigations. In fact, sample morphology is completely preserved after air drying and subjecting the particles to an argon plasma at reduced pressure.

Figure 4 (top) displays the typical particle morphology obtained from bulk sample preparations. It is seen that the spines emerging from the outer shell surface are completely stable. These hollow mineralized spines have an average diameter of some 400–600 nm, while the average wall thickness amounts to approximately 60 nm, as can be seen from scanning electron micrographs of fractured samples at high magnification (Figure 4, bottom). The elemental composition was determined at selected sample areas by using energy-dispersive X-ray (EDX) fluorescence. EDX spectra spotted at the inner droplet surface and at the surface of discrete spines confirm the presence of both Si and Ti.

While there are many reports that make use of organic templates (e.g. liquid crystalline mesophases,^[19] vesicles,^[20] polymer latex spheres,^[21] macromolecules,^[22] or oil/water microemulsions^[23]) to produce inorganic (silica) materials with well-defined porosity, our approach differs in that a dynamic dissipation process (i.e. the spontaneous emulsification of oil droplets) is used to shape the inorganic matrix.^[24] In this regard our approach is certainly related to natural biomineralization processes, although there might be only a faint relation to the various, highly specialized (macro-)molecular constituents of biosilicifying organisms. We anticipate that a closer relation may be achieved once more insight into the functional properties of these macromolecules in biological systems becomes available. Future investigations will focus on the mechanisms that govern the formation of star-shaped particle morphologies.

- [1] a) C. C. Perry, T. Keeling-Tucker, *J. Biol. Inorg. Chem.* **2000**, *5*, 537–550; b) *Silicon and Siliceous Structures in Biological Systems* (Eds.: T. L. Simpson, B. E. Volcani), Springer, New York, **1981**.
- [2] a) J. N. Cha, K. Shimizu, Y. Zhou, S. C. Christiansen, B. F. Chmelka, G. D. Stucky, D. E. Morse, *Proc. Natl. Acad. Sci. USA* **1999**, *96*, 361–365; b) K. Shimizu, J. Cha, G. D. Stucky, D. E. Morse, *Proc. Natl. Acad. Sci. USA* **1998**, *95*, 6234–6238.
- [3] a) N. Kröger, R. Deutzmann, M. Sumper, *J. Biol. Chem.* **2001**, *276*, 26066–26070; b) N. Kröger, R. Deutzmann, C. Bergsdorf, M. Sumper, *Proc. Natl. Acad. Sci. USA* **2000**, *97*, 14133–14138; c) N. Kröger, R. Deutzmann, M. Sumper, *Science* **1999**, *286*, 1129–1132.
- [4] N. Kröger, C. Bergsdorf, M. Sumper, *Eur. J. Biochem.* **1996**, *239*, 259–264.
- [5] a) N. Kröger, R. Wetherbee, *Protist* **2000**, *151*, 263–273; b) N. Kröger, G. Lehmann, R. Rachel, M. Sumper, *Eur. J. Biochem.* **1997**, *250*, 99–105.
- [6] T. F. Schultz, L. Egerton-Warburton, S. A. Crawford, R. Wetherbee, *Protist* **2001**, *152*, 315–327.
- [7] E. G. Vrieling, T. P. M. Beelen, R. A. van Santen, W. W. C. Gieskes, *J. Biotechnol.* **1999**, *70*, 39–51.
- [8] a) D. Volkmer, *Chem. Unserer Zeit* **1999**, *33*, 6–19; b) E. G. Vrieling, W. W. C. Gieskes, T. P. M. Beelen, *J. Phycol.* **1999**, *35*, 548–559.
- [9] For different working hypotheses on the mechanisms of pattern formation in diatom biosilica see: a) R. Gordon, R. W. Drum, *Int. Rev. Cytol.* **1994**, *150*, 243–372; b) A. M. M. Schmid, R. K. Eberwein, M. Hesse, *Protoplasma* **1996**, *193*, 144–173; c) E. G. Vrieling, T. P. M. Beelen, R. A. van Santen, W. W. C. Gieskes, *Angew. Chem.* **2002**, *114*, 1613–1616; *Angew. Chem. Int. Ed.* **2002**, *41*, 1543–1546; d) M. Sumper, *Science* **2002**, *295*, 2430–2433.
- [10] O. R. Anderson, *Protoplasma* **1994**, *181*, 61–77.
- [11] R. Wetherbee, S. Crawford, P. Mulvaney, *The Nanostructure and Development of Diatom Biosilica in: Biomineralization* (Ed.: E. Baeuerlein), Wiley-VCH, Weinheim, **2000**, pp. 189–205.
- [12] Chlorocyclohexane was chosen because of its specific density of 1.0 g cm⁻³, which avoids droplet buoyancy in aqueous solution.
- [13] Selected references: a) N. Shahidzadeh, D. Bonn, J. Meunier, M. Nabavi, M. Airiau, M. Morvan, *Langmuir* **2000**, *16*, 9703–9708; b) T. Nishimi, C. A. Miller, *Langmuir* **2000**, *16*, 9233–9241; c) C. A. Miller, *Colloids Surf.* **1988**, *29*, 89–102; d) O. Theissen, G. Gompper, *Eur. Phys. J. B* **1999**, *11*, 91–100; e) M. J. Rang, C. A. Miller, *J. Colloid Interface Sci.* **1999**, *209*, 179–192; f) R. Granek, R. C. Ball, M. E. Cates, *J. Phys. II* **1993**, *3*, 829–849; g) W. J. Benton, C. A. Miller, T. Fort, *J. Dispersion Sci. Technol.* **1982**, *3*, 1–44.
- [14] Mixtures of cationic and anionic surfactants often lead to spontaneous formation of (thermodynamically stable) vesicles: a) E. W. Kaler, A. K. Murthy, B. E. Rodriguez, J. A. N. Zasadzinski, *Science* **1989**, *245*, 1371–1374; b) S. A. Safran, P. Pincus, D. Andelman, *Science* **1990**, *248*, 354–355; c) C. Tondre, C. Caillet, *Adv. Colloid Interface Sci.* **2001**, *93*, 115–134.
- [15] The formation of hollow silica shells using an oil/water microemulsion template has been reported by different research groups. However, silicic acid condensation occurs under either strongly acidic or basic conditions: a) S. Schacht, Q. Huo, I. G. Voigt-Martin, G. D. Stucky, F. Schüth, *Science* **1996**, *273*, 768–771; b) C. E. Fowler, D. Khushalani, S. Mann, *Chem. Commun.* **2001**, 2028–2029.
- [16] R. J. Davis, Z. Liu, *Chem. Mater.* **1997**, *9*, 2311–2324.
- [17] T. Nielsen, M. Fricke, D. Hellweg, P. Andresen, *J. Microsc.* **2001**, *201*, 368–376.
- [18] J. H. Fuhrhop, W. Helfrich, *Chem. Rev.* **1993**, *93*, 1565–1582.
- [19] a) C. T. Kresge, M. E. Leonowicz, W. J. Roth, J. C. Vartuli, J. S. Beck, *Nature* **1992**, *359*, 710–712; b) G. S. Attard, J. C. Glyde, C. G. Göltner, *Nature* **1995**, *378*, 366–368.
- [20] a) S. S. Kim, W. Z. Zhang, T. J. Pinnavaia, *Science* **1998**, *282*, 1302–1305; b) P. T. Tanev, T. J. Pinnavaia, *Science* **1996**, *271*, 1267–1269.
- [21] a) F. Caruso, R. A. Caruso, H. Möhwald, *Science* **1998**, *282*, 1111–1114; b) B. T. Holland, C. F. Blanford, T. Do, A. Stein, *Chem. Mater.* **1999**, *11*, 795–805.
- [22] a) C. Göltner, S. Henke, M. C. Weißenberger, M. Antonietti, *Angew. Chem.* **1998**, *110*, 633–636; *Angew. Chem. Int. Ed.* **1998**, *37*, 613–616; b) J. N. Cha, G. D. Stucky, D. E. Morse, T. J. Deming, *Nature* **2000**, *403*, 289–292; c) D. Y. Zhao, J. L. Feng, Q. S. Huo, N. Melosh, G. H. Fredrickson, B. F. Chmelka, G. D. Stucky, *Science* **1998**, *279*, 548–552; d) M. Templin, A. Franck, A. DuChesne, H. Leist, Y. M. Zhang, R. Ulrich, V. Schädler, U. Wiesner, *Science* **1997**, *278*, 1795–1798.
- [23] a) S. Schacht, Q. Huo, I. G. Voigt-Martin, G. D. Stucky, F. Schüth, *Science* **1996**, *273*, 768–771; b) P. Schmidt-Winkel, W. W. Lukens Jr., P. Yang, D. I. Margolese, J. S. Lettow, J. Y. Ying, G. D. Stucky, *Chem. Mater.* **2000**, *12*, 686–696.
- [24] Dynamic transformation processes leading to complex morphologies have been reported. The precise function of the organic template, however, is in most cases not well established. Selected reviews on this subject: a) S. Mann, G. A. Ozin, *Nature* **1996**, *382*, 313–318; b) G. A. Ozin, *Acc. Chem. Res.* **1997**, *30*, 17–27; c) S. Mann, S. L. Burkett, S. A. Davis, C. E. Fowler, N. H. Mendelson, S. D. Sims, D. Walsh, N. T. Whilton, *Chem. Mater.* **1997**, *9*, 2300–2310; d) S. Mann, *Angew. Chem.* **2000**, *112*, 3532–3548; *Angew. Chem. Int. Ed.* **2000**, *39*, 3392–3406; e) L. A. Estroff, A. D. Hamilton, *Chem. Mater.* **2001**, *13*, 3227–3235.